Acta Cryst. (1996). B52, 1007–1013

Structures and Photochemistry of Dibenzobarrelene Monoamides

Ray Jones, A. Graham M. Rattray, Steven J. Rettig, John R. Scheffer and James Trotter*

Department of Chemistry, University of British Columbia, Vancouver, BC, Canada V6T 1Z1

(Received 27 March 1996; accepted 17 June 1996)

Abstract

The photochemistry of 9,10-ethenoanthracene-11-monoamides has been studied and correlated with the crystal structures determined for two derivatives; photoproduct structures have been established from a crystal structure analysis of one of the products and from NMR correlations. Crystal data are: (1)-Et, *N,N*-diethyl-9,10-dihydro-9,10-ethenoanthracene-11-carboxamide, $C_{21}H_{21}NO$, *Pbca*; (1)-Pr, 9,10-dihydro-*N,N*-di(isopropyl)-9,10-ethenoanthracene-11-carboxamide, $C_{23}H_{25}NO$, $P2_1/c$; (2*L*)-Bz, 9,10-dihydro-9,10-ethenoanthracene-11-spiro-3′-(1-benzyl-4-phenylazetidine)-2′-one, $C_{31}H_{25}NO$ (+ solvent), $P2_1/a$ ($Z = 8$). The two dibenzobarrelene molecules have geometries and dimensions similar to those of related materials; the amide group in each molecule is only partially conjugated with the C11=C12 double bond. Mechanisms are derived for the formation of three types of photoproduct: (i) the well known di-π-methane reaction [(2*M*)-type photoproduct]; (ii) a hydrogen abstraction process (2*H*); (iii) β-lactam formation (2*L*).

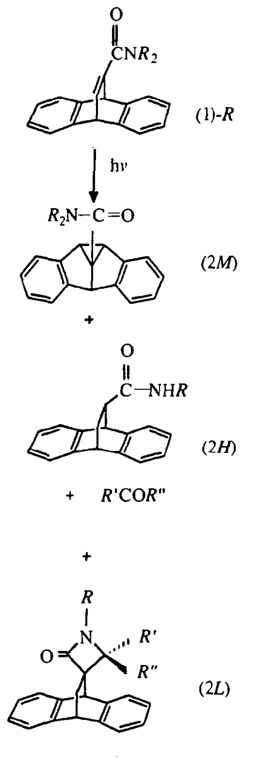

R = Et, Pr^i, Bz
R′ = Me, Me, Ph
R″ = H, Me, H

1. Introduction

Studies of the photochemistry of dibenzobarrelene derivatives (Pokkuluri, Scheffer & Trotter, 1993*a,b*; Jones, Rettig, Scheffer, Trotter & Yang, 1996) have been extended to examine the reactions of monoamides. Photolysis of these materials [(1)-*R*] in solution and in the solid state gives three types of photoproduct [(2*M*), (2*H*) and (2*L*)]. The crystal structures of two derivatives have been determined: (1)-*R*, *R* = Et, Pr^i. The molecular structure of one of the photoproducts (2*L*)-Bz was determined by crystal structure analysis, and the structures of the other photoproducts from spectroscopic (mainly NMR) data.

2. Experimental

The dibenzobarrelene monoamides were synthesized from a monocarboxylate (Rattray, 1992, see deposition material†). X-ray data, measured on a Rigaku AFC-6*S* diffractometer, are summarized in Table 1. The structures were solved by direct methods and refined by full-matrix least-squares procedures, with $w = 1/\sigma^2(F)$. H-atom parameters were fixed at calculated values. For (1)-Et, one ethyl group is disordered (occupancies 81:19; isotropic thermal parameters for the lower occupancy sites). Crystals of (1)-Bz were not suitable for X-ray analysis. For (2*L*)-Bz a region of electron-density peaks probably corresponds to solvent (the crystals were obtained from chloroform/petroleum ether), but the distribution could not be readily interpreted in terms of disordered solvent molecules. The region probably contains superimposed chloroform and hydrocarbon molecules. The largest peak in this region was modeled as a half-occupancy Cl atom, refined with anisotropic thermal parameters. All other

---

† Synthesis of materials and photochemical details, lists of structure factors, anisotropic displacement parameters, H-atom coordinates and complete geometry, and packing diagrams have been deposited with the IUCr (Reference: FG0004). Copies may be obtained through The Managing Editor, International Union of Crystallography, 5 Abbey Square, Chester CH1 2HU, England.

Table 1. *Experimental details*

	(1)-Et	(1)-Pr	(2*L*)-Bz
Crystal data			
Chemical formula	$C_{21}H_{21}NO$	$C_{23}H_{25}NO$	$C_{31}H_{25}NO.(CHCl_3)_{0.25}.(C_6H_{12})_{0.25}$
Chemical formula weight	303.40	331.46	478.43
Cell setting	Orthorhombic	Monoclinic	Monoclinic
Space group	*Pbca*	$P2_1/c$	$P2_1/a$
a (Å)	31.863 (2)	10.846 (1)	10.228 (3)
b (Å)	11.088 (2)	10.788 (2)	32.818 (3)
c (Å)	9.400 (3)	17.0463 (9)	15.529 (3)
β (°)		107.836 (7)	99.79 (2)
V (Å^3)	3320 (1)	1898.7 (4)	5137 (1)
Z	8	4	8
D_x (Mg m^{-3})	1.214	1.159	1.237
Radiation type	Cu $K\alpha$	Mo $K\alpha$	Cu $K\alpha$
Wavelength (Å)	1.5418	0.7107	1.5418
No. of reflections for cell parameters	25	25	24
θ range (°)	24.6–39.4	11.4–18.2	15.5–24.2
μ (mm^{-1})	0.574	0.065	1.265
Temperature (K)	294	294	294
Crystal form	Plate	Prism	Plate
Crystal size (mm)	0.15 × 0.15 × 0.05	0.42 × 0.37 × 0.22	0.45 × 0.20 × 0.10
Crystal color	Colorless	Colorless	Colorless
Data collection			
Diffractometer	Rigaku AFC-6*S*	Rigaku AFC-6*S*	Rigaku AFC-6*S*
Data collection method	ω–2θ scans	ω–2θ scans	ω–2θ scans
Absorption correction	ψ scans (North, Phillips & Mathews, 1968)	ψ scans (North, Phillips & Mathews, 1968)	ψ scans (North, Phillips & Mathews, 1968)
$T_{\min}$	0.984	0.942	0.754
$T_{\max}$	1.000	1.000	1.000
No. of measured reflections	3505	4833	11 174
No. of independent reflections	3505	4358	10 345
No. of observed reflections	1669	2360	4319
Criterion for observed reflections	$I > 3.00\sigma(I)$	$I > 3.00\sigma(I)$	$I > 3.00\sigma(I)$
$R_{\rm int}$	-	0.027	0.0265
$\theta_{\max}$ (°)	77.43	27.50	77.69
Range of h, k, l	$0 \rightarrow h \rightarrow 40$ $0 \rightarrow k \rightarrow 14$ $-11 \rightarrow l \rightarrow 0$	$0 \rightarrow h \rightarrow 14$ $0 \rightarrow k \rightarrow 14$ $-21 \rightarrow l \rightarrow 21$	$0 \rightarrow h \rightarrow 12$ $0 \rightarrow k \rightarrow 41$ $-19 \rightarrow l \rightarrow 19$
No. of standard reflections	3	3	3
Frequency of standard reflections	Every 150 reflections	Every 200 reflections	Every 250 reflections
Intensity decay (%)	2.9	0.3	8.6
Refinement			
Refinement on	F	F	F
R	0.0398	0.0372	0.0471
wR	0.0331	0.0336	0.0411
S	1.946	2.227	2.410
No. of reflections used in refinement	1669	2360	4319
No. of parameters used	227	227	649
H-atom treatment	C—H riding	C—H riding	C—H riding
Weighting scheme	$w = 1/[\sigma^2(F_o)]$	$w = 1/[\sigma^2(F_o)]$	$w = 1/[\sigma^2(F_o)]$
$(\Delta/\sigma)_{\max}$	0.009	0.0003	0.0660
$\Delta\rho_{\max}$ (e Å^{-3})	0.13	0.19	0.31
$\Delta\rho_{\min}$ (e Å^{-3})	−0.18	−0.12	−0.30
Extinction method	Zachariasen (1967)	Zachariasen (1967)	Zachariasen (1967)
Extinction coefficient	0.97 (7) × 10^{-6}	0.89 (4) × 10^{-6}	0.54 (5) × 10^{-6}
Source of atomic scattering factors	*International Tables for Crystallography* (1992, Vol. C, Table 6.1.1.2)	*International Tables for Crystallography* (1992, Vol. C, Table 6.1.1.2)	*International Tables for Crystallography* (1992, Vol. C, Table 6.1.1.2)
Computer programs			
Data collection	*MSC/AFC* (Molecular Structure Corporation, 1988)	*MSC/AFC* (Molecular Structure Corporation, 1988)	*MSC/AFC* (Molecular Structure Corporation, 1988)
Cell refinement	*MSC/AFC* (Molecular Structure Corporation, 1988)	*MSC/AFC* (Molecular Structure Corporation, 1988)	*MSC/AFC* (Molecular Structure Corporation, 1988)
Data reduction	*TEXSAN* (Molecular Structure Corporation, 1995)	*TEXSAN* (Molecular Structure Corporation, 1995)	*TEXSAN* (Molecular Structure Corporation, 1993)
Structure solution	*SIR*92 (Altomare *et al.*, 1993)	*SIR*92 (Altomare *et al.*, 1993)	*SIR*92 (Altomare *et al.*, 1993)
Structure refinement	*TEXSAN* (Molecular Structure Corporation, 1995)	*TEXSAN* (Molecular Structure Corporation, 1995)	*TEXSAN* (Molecular Structure Corporation, 1993)
Preparation of material for publication	*TEXSAN* (Molecular Structure Corporation, 1995)	*TEXSAN* (Molecular Structure Corporation, 1995)	*TEXSAN* (Molecular Structure Corporation, 1993)

Table 2. *Fractional atomic coordinates and equivalent isotropic displacement parameters* ($\AA^2$)

$$U_{eq} = (1/3)\Sigma_i\Sigma_j U_{ij}a_i^*a_j^*\mathbf{a}_i.\mathbf{a}_j.$$

	x	y	z	U_{eq}
(1)-Et				
O(1)	0.28809 (5)	0.4193 (2)	0.4627 (2)	0.0821 (7)
N(1)	0.29502 (6)	0.2186 (2)	0.4916 (3)	0.0668 (8)
C(1)	0.43226 (8)	0.4751 (2)	0.6676 (3)	0.0503 (8)
C(2)	0.47247 (8)	0.4423 (2)	0.7108 (3)	0.0569 (9)
C(3)	0.49739 (8)	0.3711 (3)	0.6252 (3)	0.0583 (9)
C(4)	0.48269 (7)	0.3313 (2)	0.4943 (3)	0.0542 (8)
C(4a)	0.44287 (7)	0.3643 (2)	0.4505 (3)	0.0431 (7)
C(5)	0.42665 (8)	0.5018 (3)	0.1135 (3)	0.0581 (9)
C(6)	0.4157 (1)	0.6179 (3)	0.0715 (3)	0.071 (1)
C(7)	0.3907 (1)	0.6879 (3)	0.1577 (4)	0.071 (1)
C(8)	0.37591 (8)	0.6445 (2)	0.2872 (3)	0.0575 (9)
C(8a)	0.38711 (7)	0.5294 (2)	0.3299 (3)	0.0451 (7)
C(9)	0.37565 (7)	0.4667 (2)	0.4688 (3)	0.0430 (7)
C(9a)	0.41774 (7)	0.4360 (2)	0.5377 (3)	0.0419 (7)
C(10)	0.42216 (7)	0.3364 (2)	0.3083 (3)	0.0463 (8)
C(10a)	0.41251 (7)	0.4588 (2)	0.2426 (3)	0.0456 (7)
C(11)	0.35548 (7)	0.3460 (2)	0.4268 (3)	0.0429 (7)
C(12)	0.37982 (7)	0.2801 (2)	0.3429 (3)	0.0473 (8)
C(13)	0.31067 (8)	0.3289 (2)	0.4636 (3)	0.0554 (8)
C(14)	0.2483 (1)	0.2071 (3)	0.5040 (5)	0.061 (1)
C(14′)	0.2602 (5)	0.209 (2)	0.623 (3)	0.075 (7)
C(15′)	0.2183 (5)	0.203 (1)	0.539 (3)	0.107 (8)
C(15)	0.2362 (2)	0.2280 (6)	0.6517 (7)	0.110 (2)
C(16)	0.31953 (8)	0.1093 (2)	0.5133 (4)	0.0694 (10)
C(17)	0.31456 (10)	0.0202 (3)	0.3928 (4)	0.091 (1)
(1)-Pr				
O(1)	0.3259 (1)	0.1516 (1)	0.46957 (8)	0.0542 (4)
N(1)	0.2272 (1)	0.1342 (1)	0.33230 (8)	0.0375 (4)
C(1)	0.6100 (2)	0.4770 (2)	0.4394 (1)	0.0478 (7)
C(2)	0.7248 (2)	0.5202 (2)	0.4944 (1)	0.0585 (8)
C(3)	0.8307 (2)	0.4434 (2)	0.5207 (1)	0.0540 (7)
C(4)	0.8242 (2)	0.3215 (2)	0.4932 (1)	0.0445 (6)
C(4a)	0.7102 (2)	0.2782 (2)	0.4381 (1)	0.0349 (5)
C(5)	0.7136 (2)	0.1395 (2)	0.2504 (1)	0.0516 (7)
C(6)	0.6718 (2)	0.1810 (2)	0.1693 (1)	0.0633 (8)
C(7)	0.5685 (2)	0.2614 (2)	0.1429 (1)	0.0645 (8)
C(8)	0.5037 (2)	0.3009 (2)	0.1968 (1)	0.0513 (7)
C(8a)	0.5443 (2)	0.2599 (2)	0.2777 (1)	0.0383 (5)
C(9a)	0.6033 (2)	0.3568 (2)	0.4110 (1)	0.0362 (5)
C(9)	0.4895 (2)	0.2967 (2)	0.3465 (1)	0.0369 (5)
C(10)	0.6850 (2)	0.1516 (2)	0.3969 (1)	0.0367 (5)
C(10a)	0.6502 (2)	0.1798 (2)	0.3048 (1)	0.0381 (5)
C(11)	0.4605 (2)	0.1760 (2)	0.38501 (10)	0.0335 (5)
C(12)	0.5628 (2)	0.1025 (2)	0.4119 (1)	0.0358 (5)
C(13)	0.3321 (2)	0.1518 (2)	0.3987 (1)	0.0359 (5)
C(14)	0.0981 (2)	0.1169 (2)	0.3436 (1)	0.0470 (6)
C(15)	0.2352 (2)	0.1221 (2)	0.2477 (1)	0.0468 (6)
C(16)	0.0558 (2)	0.2311 (2)	0.3806 (2)	0.0791 (9)
C(17)	0.0903 (2)	−0.0002 (3)	0.3906 (2)	0.0802 (9)
C(18)	0.1637 (2)	0.2261 (2)	0.1921 (1)	0.0741 (8)
C(19)	0.1893 (2)	−0.0046 (2)	0.2114 (1)	0.0632 (7)
(2*L*)-Bz				
Cl(1)	0.4432 (5)	0.3372 (2)	0.2339 (2)	0.210 (2)
O(1)	0.4751 (2)	0.68503 (8)	0.1639 (2)	0.075 (1)
O(2)	−0.0518 (2)	0.47530 (8)	0.2198 (2)	0.0678 (9)
N(1)	0.6971 (3)	0.70515 (9)	0.1732 (2)	0.056 (1)
N(2)	0.1541 (3)	0.50799 (8)	0.2438 (2)	0.0475 (9)
C(1)	0.8230 (3)	0.6168 (1)	−0.0651 (2)	0.045 (1)
C(2)	0.9071 (3)	0.5856 (1)	−0.0805 (2)	0.052 (1)
C(3)	0.9060 (3)	0.5493 (1)	−0.0377 (2)	0.053 (1)
C(4)	0.8205 (3)	0.5424 (1)	0.0214 (2)	0.050 (1)
C(4a)	0.7354 (3)	0.5732 (1)	0.0366 (2)	0.042 (1)
C(5)	0.3880 (4)	0.5580 (1)	0.0247 (2)	0.058 (1)
C(6)	0.2763 (4)	0.5721 (1)	−0.0305 (3)	0.069 (2)
C(7)	0.2771 (3)	0.6096 (1)	−0.0701 (3)	0.067 (1)
C(8)	0.3901 (4)	0.6337 (1)	−0.0558 (2)	0.055 (1)
C(8a)	0.5016 (3)	0.6197 (1)	−0.0016 (2)	0.044 (1)
C(9)	0.6354 (3)	0.64071 (9)	0.0170 (2)	0.041 (1)
C(9a)	0.7357 (3)	0.61051 (10)	−0.0072 (2)	0.039 (1)
C(10)	0.6318 (3)	0.57108 (10)	0.0947 (2)	0.046 (1)
C(10a)	0.5007 (3)	0.5818 (1)	0.0395 (2)	0.044 (1)
C(11)	0.6689 (3)	0.64714 (10)	0.1173 (2)	0.044 (1)
C(12)	0.6645 (3)	0.6055 (1)	0.1637 (2)	0.053 (1)
C(13)	0.7928 (3)	0.6751 (1)	0.1516 (2)	0.048 (1)
C(15)	0.5894 (4)	0.6810 (1)	0.1533 (2)	0.054 (1)
C(16)	0.8833 (3)	0.6897 (1)	0.0917 (2)	0.046 (1)
C(17)	1.0045 (4)	0.6712 (1)	0.0938 (3)	0.062 (1)
C(18)	1.0887 (4)	0.6829 (2)	0.0383 (4)	0.087 (2)
C(19)	1.0521 (6)	0.7129 (2)	−0.0216 (4)	0.100 (2)
C(20)	0.9330 (6)	0.7327 (1)	−0.0236 (3)	0.097 (2)
C(21)	0.8484 (4)	0.7212 (1)	0.0332 (3)	0.070 (1)
C(22)	0.7216 (4)	0.7410 (1)	0.2287 (3)	0.064 (1)
C(23)	0.7883 (4)	0.7300 (1)	0.3198 (3)	0.057 (1)
C(24)	0.7354 (4)	0.7004 (1)	0.3676 (3)	0.072 (2)
C(25)	0.7973 (6)	0.6903 (1)	0.4504 (4)	0.088 (2)
C(26)	0.9126 (6)	0.7092 (2)	0.4865 (3)	0.100 (2)
C(27)	0.9671 (5)	0.7384 (2)	0.4391 (4)	0.106 (2)
C(28)	0.9044 (5)	0.7487 (1)	0.3561 (3)	0.077 (2)
C(31)	0.4093 (4)	0.3986 (1)	0.4366 (3)	0.067 (1)
C(32)	0.4818 (4)	0.3938 (1)	0.5209 (3)	0.083 (2)
C(33)	0.4260 (5)	0.4026 (1)	0.5924 (3)	0.087 (2)
C(34)	0.2969 (5)	0.4162 (1)	0.5839 (3)	0.074 (2)
C(34a)	0.2233 (4)	0.4206 (1)	0.5018 (3)	0.057 (1)
C(35)	−0.1160 (5)	0.3869 (2)	0.4316 (3)	0.088 (2)
C(36)	−0.1760 (5)	0.3591 (2)	0.3702 (4)	0.114 (2)
C(37)	−0.1194 (6)	0.3492 (2)	0.2993 (4)	0.106 (2)
C(38)	−0.0004 (5)	0.3672 (1)	0.2859 (3)	0.078 (2)
C(38a)	0.0589 (4)	0.3954 (1)	0.3471 (3)	0.058 (1)
C(39)	0.1847 (4)	0.4190 (1)	0.3423 (2)	0.050 (1)
C(39a)	0.2786 (4)	0.4118 (1)	0.4273 (3)	0.054 (1)
C(40)	0.0816 (4)	0.4354 (1)	0.4794 (2)	0.061 (1)
C(40a)	0.0033 (4)	0.4046 (1)	0.4201 (3)	0.063 (1)
C(41)	0.1462 (3)	0.4648 (1)	0.3415 (2)	0.047 (1)
C(42)	0.0854 (4)	0.4746 (1)	0.4235 (2)	0.063 (1)
C(43)	0.2520 (3)	0.49673 (10)	0.3202 (2)	0.046 (1)
C(45)	0.0603 (4)	0.4811 (1)	0.2580 (2)	0.049 (1)
C(46)	0.3849 (3)	0.48359 (10)	0.3007 (2)	0.046 (1)
C(47)	0.4985 (4)	0.4909 (1)	0.3600 (3)	0.069 (1)
C(48)	0.6206 (4)	0.4784 (1)	0.3422 (3)	0.090 (2)
C(49)	0.6309 (4)	0.4592 (1)	0.2660 (3)	0.086 (2)
C(50)	0.5185 (4)	0.4520 (1)	0.2063 (3)	0.074 (2)
C(51)	0.3961 (3)	0.4642 (1)	0.2233 (2)	0.057 (1)
C(52)	0.1494 (3)	0.5431 (1)	0.1870 (2)	0.054 (1)
C(53)	0.1539 (3)	0.5823 (1)	0.2376 (2)	0.048 (1)
C(54)	0.0573 (4)	0.5907 (1)	0.2882 (3)	0.062 (1)
C(55)	0.0599 (5)	0.6266 (1)	0.3336 (3)	0.076 (2)
C(56)	0.1605 (6)	0.6544 (1)	0.3310 (3)	0.085 (2)
C(57)	0.2562 (4)	0.6464 (1)	0.2815 (3)	0.076 (2)
C(58)	0.2528 (4)	0.6107 (1)	0.2341 (3)	0.062 (1)
C(59)	0.282 (2)	0.2641 (6)	0.325 (2)	0.185 (8)
C(60)	0.520 (4)	0.302 (2)	0.264 (3)	0.17 (1)
C(61)	0.555 (1)	0.2654 (4)	0.2835 (7)	0.167 (4)
C(62)	0.336 (2)	0.2930 (5)	0.3525 (10)	0.191 (5)
C(63)	0.439 (3)	0.2669 (9)	0.218 (2)	0.18 (1)
C(65)	0.402 (2)	0.3029 (5)	0.283 (1)	0.187 (6)
C(66)	0.489 (1)	0.2886 (3)	0.3646 (7)	0.188 (4)
C(67)	0.240 (1)	0.2731 (5)	0.258 (1)	0.184 (6)
C(68)	0.303 (2)	0.2787 (4)	0.2032 (9)	0.192 (5)
C(69)	0.272 (2)	0.3075 (7)	0.292 (2)	0.187 (8)
C(70)	0.438 (3)	0.2557 (9)	0.289 (2)	0.19 (1)

solvent region peaks were refined as C atoms with isotropic thermal parameters. Occupancy factors were adjusted as the refinement progressed to yield approximately equal thermal parameters.

Scattering factors were from the *International Tables for Crystallography* (1992), computer programs as supplied in *TEXSAN* (Molecular Structure Corporation, 1995). Details of the refinements are given in Table 1.

Table 3. *Selected bond lengths (Å) and angles (°)*

	(1)-Et	(1)-Pr	(2*L*)-Bz
C11=C12	1.326 (3)	1.326 (2)	[1.549, 1.544 (4)]
C=O	1.233 (3)	1.230 (2)	1.215, 1.214 (4)
OC—N	1.348 (3)	1.350 (2)	1.349, 1.349 (4)
C—C—C (ring junction, external)	126.8-127.4 (2)	126.7-127.7 (2)	125.6-126.9 (4)
Angles in 4-ring:			
at N	-	-	96.0, 96.3 (3)
at C	-	-	84.3-92.6 (3)

3. Discussion

Final positional parameters are given in Table 2, selected molecular parameters in Table 3 and other data have been deposited.*

The two dibenzobarrelene molecules have geometries and dimensions (Fig. 1 and Table 3) similar to those of related materials (Pokkuluri *et al.*, 1993*a*,*b*; Jones *et al.*, 1996). The external angles at the ring junctions are increased to ~127° (Table 3) as a result of ring junction strain. The amide groups are only partially conjugated with the C11=C12 double bond, the C=C—C=O torsion angles being −136.0(3) and 63.8(3)° for the (1)-Et and (1)-Pr compounds, respectively [$\cos^2$(angle) = 0.52 and 0.19].

The molecular structures of the di-π-methane photoproducts (2*M*) were established from NMR data and comparison with related materials (Ciganek, 1966; Jones *et al.*, 1996). Briefly, the observation of two singlets in the ratio 2:1 in the region δ 3.5-4.8 p.p.m. establishes the symmetrical location of the amide group at the (8*c*) position (semibullvalene numbering system). The structures of the photoproducts of the type (2*H*) were determined from spectroscopic data (Rattray, 1992). The parent ion peaks in the mass spectra correspond to a loss of *R*-3H mass units from the starting materials. In addition, the most intense peaks in the spectra at *m*/*z* 178 can be attributed to anthracene, typical of dibenzobarrelene, rather than semibullvalene ring systems. The strong IR absorptions at 3248, 1639 and 1535 cm^{-1} (for *R* = Et) indicate the presence of a secondary amide attached to a saturated carbon atom. Finally, the NMR spectra can be fully assigned on the basis of structure (2*H*) (Rattray, 1992).

The structure of the (2*L*)-type photoproduct, which is found mainly in the photolysis of the benzyl derivative, was established by X-ray analysis of photoproduct (2*L*)-Bz (Fig. 1). The spectroscopic data are fully consistent with this structure (Rattray, 1992). The molecule contains a dibenzobarrelene ring skeleton, with a spiro-fused β-lactam almost planar four-membered ring [mean torsion angles 5.7 (2) and 0.5 (2)° in the two independent molecules].

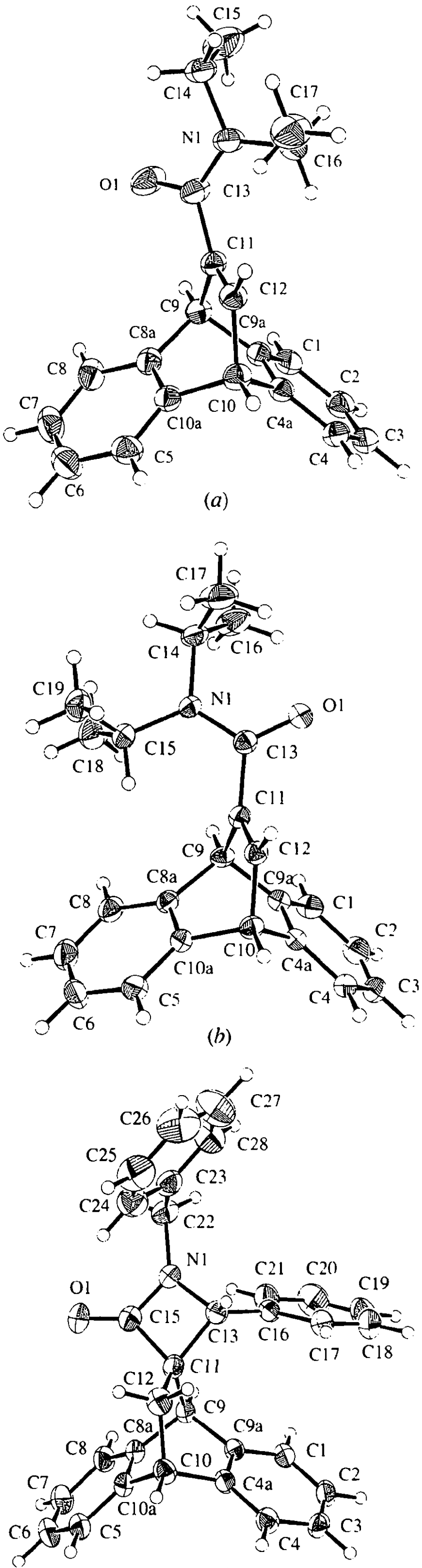

Fig. 1. Views of the molecules of (*a*) (1)-Et, (*b*) (1)-Pr and (*c*) (2*L*)-Bz (one of the two molecules in the asymmetric unit; the other is similar); 33% thermal probability ellipsoids.

---

* See deposition footnote on p. 1007.

Table 4. *Ratios of photoproducts (%)*

	Product ratios		
	(2*M*)	(2*H*)	(2*L*)
R = H or Me			
Solution or solid state	100	0	0
R = Et			
Benzene	66	33	0
Acetone, acetonitrile	75	25	0
Solid state	100	0	0
R = Pr^i			
Benzene	30	60	10
Acetone	60	25	15
Acetonitrile	30	60	10
Solid state	100	0	0
R = $\mathrm{CH_2Ph}$ (Bz)			
Benzene	35	5	60
Acetone	40	5	55
Acetonitrile	50	Trace	50
Solid state	85	0	15

3.1. *Photochemistry*

The monoamides (1)-*R* undergo the di-π-methane reaction in solution and in the solid state to produce the usual semibullvalene-type photoproducts (2*M*). These are the major products in the solid-state photolysis, but in solution significant amounts of two other products are found, (2*H*) and (2*L*) (Table 4).

In the di-π-methane rearrangement of the dibenzobarrelene monoamides only one of two possible regioisomeric products is formed, similar to the situation in the photolysis of a monocarboxylate (Ciganek, 1966). The accepted mechanism for the di-π-methane photochemical reaction in ethenoanthracenes involves initial vinyl-benzo carbon–carbon bond formation (Zimmerman, 1991). Although there are two possible pathways, A and B (Fig. 2), the reaction is likely to proceed by the route which allows maximum π-delocalization in the intermediate biradicals, extending onto the substituent group, *i.e.* path A, producing the observed photoproduct (2*M*-A) (Fig. 2).

Photolysis of compounds (1)-*R*, *R* = H, Me, produces only photoproducts of the type (2*M*), in solution and in the solid state (Table 4). For *R* = Et, Pr^i, Bz, (2*M*) is also the only photoproduct in the solid-state photolyses (apart from a small amount of an additional product when *R* = Bz, see Table 4). In solution photolysis for *R* = Et, Pr^i, Bz, two other types of photoproduct are found, (2*H*) and (2*L*) (Table 4).

Formation of photoproducts of the type (2*H*) from reactants (1)-*R* involves reduction of the bridging double bond, with a concomitant loss of one of the amide substituent groups (Et, Pr^i or Bz). A plausible mechanism for this reaction is *via* intramolecular hydrogen abstraction by the vinylic C atom *beta* to the amide group (as shown for *R* = Et in Fig. 3), and an example of a type II reaction of an aliphatic olefin. This type of reaction has been observed previously in photocyclization of dialkylamides (Aoyama, Hasegawa, Okazaki & Omote, 1979), although the *N*,*N*-diethylamides in that case did not give rise to *N*-monosubstituted amides. After hydrogen abstraction, cleavage of a C—N bond of the resulting biradical leads to fragmentation to ketene and imine. The imine is readily hydrolysed to amine, which can then react directly with the ketene to give the secondary amide, (2*H*) (Fig. 3). Additional evidence for the validity of the proposed mechanism is obtained by photolyzing (1)-Et in benzene solution in a sealed NMR tube; the proton NMR spectrum of the photomixture exhibits peaks at δ 2.20 and 9.80 p.p.m., indicating the presence of acetyaldehyde, as required by the mechanism. Furthermore, photolysis in methanol solvent results in no production of (2*H*)-type products, but another (minor) photoproduct, which proved to be a saturated-bridge methyl ester [methyl 9,10-dihydro-9,10-ethanoanthracene-11-carboxylate, a known compound (Hill & Newkome, 1969)], formed as a result of nucleophilic trapping of the methanol solvent by the ketene intermediate. NMR and mass spectral data for the photoproducts (2*H*) and the saturated-bridge methyl ester show many similarities, additional evidence for the assignment of the (2*H*) structures.

The hydrogen abstraction reaction involves a six-membered transition state (Fig. 3), with some critical parameters: the C· · ·H distance (*d*), the angle which the C· · ·H vector makes with the plane of the C=C bond

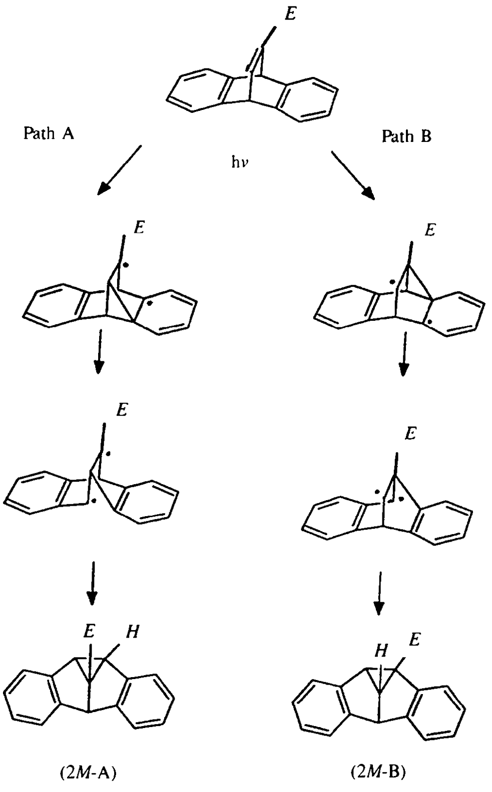

(2*M*-A) (2*M*-B)

Fig. 2. Di-π-methane mechanism.

(ω) and the C=C···H angle (Δ). Since the abstraction is *via* the *p*-orbital of the C atom, optimum values are (Trotter, 1983): $d \leq 2.9$ Å (sum of van der Waals radii), $\omega = 90°$, $\Delta = 90°$. The abstractable H atoms in (1)-Et and (1)-Pr are reasonably well sited above the C=C bonds (Fig. 1), with C···H distances of 2.55 Å (C12···H on C16) for (1)-Et and 3.14 Å (C12···H on C15) for (1)-Pr. Although the C···H distance for (1)-Et is favorable for abstraction, no hydrogen abstraction products (2*H*) are formed in any of the solid-state photolyses (Table 4); presumably subsequent steps of the reaction are inhibited in the solid-state environment. Production of (2*H*)-type products in solution photolyses presumably results from conformers with short C···H distances, the subsequent reaction steps then being feasible in solution.

Photolysis of (1)-Bz produces some di-π-methane semibullvalene photoproduct [(2*M*)-Bz] and trace amounts of the hydrogen abstraction product [(2*H*)-Bz], but the major product of solution photolysis is the ring-fused β-lactam (2*L*)-Bz (Fig. 1, Table 4). Some (2*L*)-type product is also formed from (1)-Pr. There are two mechanistic possibilities for the formation of the β-lactam (Fig. 4), both involving, as the first step, the same hydrogen abstraction process as in the production of (2*H*)-type photoproducts (Fig. 3). The second step could then be a simple ring closure, or *via* a ketene intermediate, as in (2*H*) production. The latter mechanism (*i.e.* ketene intermediate) is certainly operative, since small amounts of the (2*H*) photoproduct are obtained. More informative is the fact that photolysis in methanol solution results in the formation of the saturated-bridge methyl ester (by trapping of ketene) and no lactam is produced. Hence, the mechanism for the formation of (2*L*)-type products is most likely that involving the reaction of the ketene intermediate and an imine, a process which has been previously documented (Kirmse, 1959). The decreasing amounts of (2*L*)-type photoproduct in the series *R* = Bz, Pr^i, Et depend on the relative stabilities of the imines involved (Fig. 4). The aromatic imine that results from the irradiation of the dibenzyl compound, (1)-Bz, is most stable to hydrolysis and undergoes cycloaddition to give (2*L*)-Bz at a faster rate than hydrolysis and amine attack on the ketene [to give (2*H*)-Bz]. The rate of hydrolysis of the diethyl-derived imine is probably too large for any significant production of the β-lactam [(2*L*)-Et]. The diisopropyl

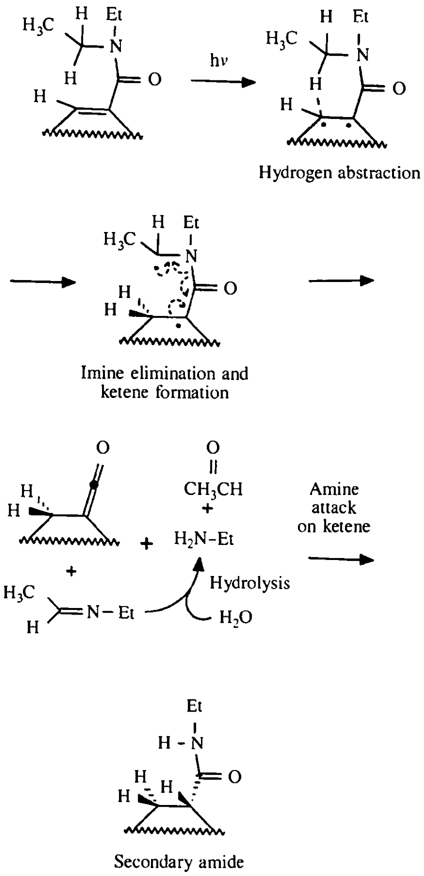

(2*H*)-Et

Fig. 3. Hydrogen abstraction mechanism.

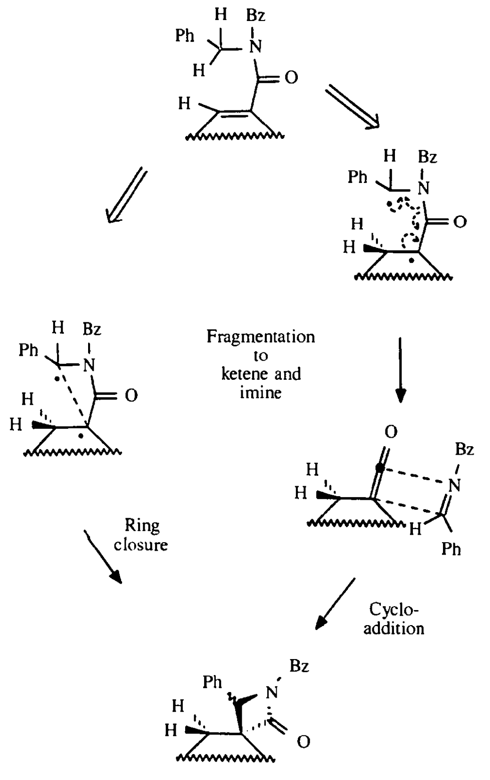

(2*L*)-Bz

Fig. 4. Mechanism for β-lactam formation.

compound (2)-Pr produces only small amounts of lactam (2*L*)-Pr, suggesting that the rate of ketene attack by the imine is less than the rate of hydrolysis of the imine. The formation of 15% of (2*L*)-Bz in the solid-state photolysis of (1)-Bz suggests that the (1)-Bz molecule exists in the crystal with a conformation which permits hydrogen abstraction (C···H ≤ 2.9 Å); unfortunately, crystals of (1)-Bz suitable for X-ray analysis could not be obtained.

We thank the Natural Sciences and Engineering Research Council of Canada for financial support.

References

Altomarc, A., Cascarano, G., Giacovazzo, C., Guagliardi, A., Burla, M. C., Polidori, G. & Camalli, M. (1994). *J. Appl. Cryst.* **27**, 435.

Aoyama, H., Hasegawa, T., Okazaki, M. & Omote, Y. (1979). *J. Chem. Soc. Perkin Trans. 1*, pp. 263–265.

Ciganek, E. (1966). *J. Am. Chem. Soc.* **88**, 2882–2883.

Hill, R. K. & Newkome, G. R. (1969). *J. Org. Chem.* **34**, 740–741.

Jones, R., Rettig, S. J., Scheffer, J. R., Trotter, J. & Yang, J. (1996). *Acta Cryst.* B**52**, 151–158.

Kirmse, W. (1959). *Angew. Chem.* **71**, 537–541.

Molecular Structure Corporation (1988). *MSC/AFC Diffractometer Control Software*. MSC 3200, Research Forest Drive, The Woodlands, TX 77381, USA.

Molecular Stucture Corporation (1995). *TEXSAN. Single Crystal Analysis Software*. Version 1.7. MSC, 3200 Research Forest Drive, The Woodlands, TX 77381, USA.

North, A. C. T., Phillips, D. C. & Mathews, F. S. (1968). *Acta Cryst.* A**24**, 351–359.

Pokkuluri, P. R., Scheffer, J. R. & Trotter, J. (1993*a*). *Acta Cryst.* B**49**, 107–116.

Pokkuluri, P. R., Scheffer, J. R. & Trotter, J. (1993*b*). *Acta Cryst.* B**49**, 754–760.

Rattray, A. G. M. (1992). Ph.D. Thesis. University of British Columbia, Vancouver, Canada.

Trotter, J. (1983). *Acta Cryst.* B**39**, 373–381.

Zachariasen, W. H. (1967). *Acta Cryst.* **23**, 558–564.

Zimmerman, H. E. (1991). *Organic Photochemistry*, edited by A. Padwa, Vol. 1, Ch. 1. New York: Marcel Dekker.